



NLR-TP-99064

Unsteady leading edge suction effects on rotor-stator interaction noise

J.B.H.M. Schulten

The contents of this report have been initially prepared for publication as AIAA paper 99-1951 in the Proceedings of the 5th AIAA/CEAS Aeroacoustics Conference, Greater Seattle, Washington, USA, 10-12 May 1999.

The contents of this report may be cited on condition that full credit is given to NLR and the author.

Division:	Fluid Dynamics
Issued:	12 February 1999
Classification of title:	Unclassified

DOCUMENT CONTROL SHEET

	ORIGINATOR'S REF. NLR-TP-99064		SECURITY CLASS. Unclassified										
ORIGINATOR National Aerospace Laboratory NLR, Amsterdam, The Netherlands													
TITLE Unsteady leading edge suction effects on rotor-stator interaction noise													
PUBLISHED IN as AIAA paper 99-1951 in the proceedings of the 5th AIAA/CEAS Aeroacoustics Conference, Greater Seattle, Washington, USA, 10-12 May 1999													
AUTHORS J.B.H.M. Schulten		DATE Feb.1999	<table style="width: 100%; border: none;"> <tr> <td style="text-align: right;">pp</td> <td style="text-align: right;">ref</td> </tr> <tr> <td style="text-align: right;">10</td> <td style="text-align: right;">11</td> </tr> </table>	pp	ref	10	11						
pp	ref												
10	11												
DESCRIPTORS <table style="width: 100%; border: none;"> <tr> <td style="width: 50%;">Aerocoustics</td> <td>Noise prediction (aircraft)</td> </tr> <tr> <td>Aerodynamic noise</td> <td>Rotor aerodynamic</td> </tr> <tr> <td>Engine noise</td> <td>Rotor blades (turbomachinery)</td> </tr> <tr> <td>Euler equations of motion</td> <td>Rotor stator interactions</td> </tr> <tr> <td>Leading edges</td> <td>Suction</td> </tr> </table>				Aerocoustics	Noise prediction (aircraft)	Aerodynamic noise	Rotor aerodynamic	Engine noise	Rotor blades (turbomachinery)	Euler equations of motion	Rotor stator interactions	Leading edges	Suction
Aerocoustics	Noise prediction (aircraft)												
Aerodynamic noise	Rotor aerodynamic												
Engine noise	Rotor blades (turbomachinery)												
Euler equations of motion	Rotor stator interactions												
Leading edges	Suction												
ABSTRACT A strictly linear analysis of the sound generated by an unleaned stator yields a vanishing amplitude for models with zero circumferential periodicity. In such a case higher order effects become relevant. In the present study the higher order effect of stator leading edge suction on radiated sound is addressed. By a local analysis in the vicinity of the leading edge a suction force can be restored from the first order theory. This suction force oscillates at twice the frequency of the associated blade loading. Numerical examples show that the effect provides a realistic floor level for the sound that otherwise would seem to vanish. For non-zero circumferential modal wave numbers the effect can increase the acoustic intensity by as much as 10dB.													



Contents

Summary	3
Nomenclature	3
Introduction	3
Theoretical modeling	4
Parametric study	6
Concluding remarks	8
References	8

1 Table

11 Figures

(10 pages in total)

Unsteady Leading Edge Suction Effects on Rotor-Stator Interaction Noise

Johan B.H.M. Schulten*

National Aerospace Laboratory NLR, 8300 AD Emmeloord, The Netherlands

A strictly linear analysis of the sound generated by an unleaned stator yields a vanishing amplitude for modes with zero circumferential periodicity. In such a case higher order effects become relevant. In the present study the higher order effect of stator leading edge suction on radiated sound is addressed. By a local analysis in the vicinity of the leading edge a suction force can be restored from the first order theory. This suction force oscillates at twice the frequency of the associated blade loading. Numerical examples show that the effect provides a realistic floor level for the sound that otherwise would seem to vanish. For non-zero circumferential modal wave numbers the effect can increase the acoustic intensity by as much as 10 dB.

Nomenclature

B	number of blades or vanes in row considered
$c(\rho)$	blade (or vane) chord
C_s	suction force coefficient [Eq.(13)]
$D(r)$	angular position of zeroth vane, [Eq.(4)]
\tilde{G}	Green's function [Eq.(3)]
h	hub/tip ratio
$\hat{i}_x, \hat{i}_r, \hat{i}_\theta$	unit vectors in x, r, θ directions
k	circumferential periodicity of incident velocity
M	axial flow Mach number
p	pressure induced by blade row
r	radial coordinate
t	time coordinate
U	local parallel flow velocity [Eq.(6)]
$U_{m\mu}$	radial eigenfunction [Eq.(4)]
v	velocity induced by blade row
w	wake velocity
x	axial coordinate along duct axis
β	$\sqrt{1 - M^2}$
γ	circulation [Eq.(6)]
Δp	blade pressure jump distribution [Eq.(4)]
$\varepsilon_{m\mu}$	radial eigenvalue [Eq.(5)]
θ	circumferential coordinate
Λ	local leading edge sweep angle
ξ	source position vector
ξ	axial source coordinate
ρ	radial source coordinate, mass density
τ	source time [Eq.(3)]

ϕ	circumferential source coordinate, argument, phase angle
ω	Helmholtz number (nondimensional frequency)

Subscripts

$(\)_L$	leading edge
$(\)_m$	merging
$(\)_s$	suction
$(\)_T$	trailing edge
$(\)_w$	wake
$(\)_\infty$	at infinity

Superscripts

$(\)^{(a)}$	anechoic
$(\)^+$	blade lower side, downstream
$(\)^-$	blade upper side, upstream
$(\)$	in physical domain

Other Symbol

$\langle \cdot \rangle$	inner product of three-dimensional vectors
-------------------------	--

Introduction

Probably the most important step forward in the history of fan noise research has been Tyler and Sofrin's¹ study on the role of blade and vane numbers in noise generation. They showed that for a fan rotating with a subsonic tip speed it is straightforward to suppress the fundamental blade passing frequency (1st harmonic) by choosing a sufficiently high number of stator vanes. Then, all acoustic duct modes become cut-off and do not propagate along the duct. In aeronautical practice "sufficiently high" turns out to be about twice the number of rotor blades.

*Senior Research Engineer, Aeroacoustics Department, P.O. Box 153. E-mail: schulten@nlr.nl. Senior Member AIAA.

In an idealized model the duct mean flow is uniform and the acoustic perturbations are small. Corresponding blade rows are aligned with the relative mean flow and thus lack mean loading. Then, the expression for the modal amplitudes generated by the impingement of rotor wakes on a stator shows that amplitudes are proportional to the circumferential mode number m . According to Tyler and Sofrin's selection rule we obtain $m=0$ in the 2nd harmonic when the stator vane number is exactly twice the rotor blade number. This would result in a zero amplitude. Of course, this looks too good to be true and, as shown earlier², higher order effects such as realistic vane camber and stagger angle become significant under such circumstances. However, even with an idealized geometry the acoustic intensity will not vanish. This is because of another nonlinear, higher order phenomenon: the presence of a vane leading edge suction force, oscillating with the incident flow distortions. The present paper analyzes this mechanism and computes its acoustic effects.

Theoretical modeling

Governing equations

In the present study a lifting surface, i.e. linearized and inviscid, modeling of the rotor-wake/stator interaction will be used. A lifting surface modeling of a flow problem is based on two assumptions. First, the viscosity of the flow is considered to be small, i.e. the Reynolds number is assumed to be sufficiently high. Secondly, the perturbations of the main flow caused by the presence of the blades are supposed to be relatively small.

We consider a single blade row placed in a uniform, subsonic main flow of Mach number M ($0 < M < 1$). To obtain a non-dimensional formulation, the mass density and speed of sound of the main flow and the duct radius are taken as scaling parameters. With this scaling the pressure and density perturbation become to leading order identical. If the x -axis is chosen along the duct axis, the governing, i.e. the leading order, flow equations are the linearized Euler equations for the (dimensionless) perturbation pressure \bar{p} and velocity \bar{v}

$$\frac{D\bar{p}}{Dt} + \langle \nabla \cdot \bar{v} \rangle = 0 \quad (1)$$

and

$$\frac{D\bar{v}}{Dt} + \nabla\bar{p} = 0 \quad (2)$$

where the linearized material derivative $D/Dt =$

$\partial/\partial t + M\partial/\partial x$. A tilde indicates that the variable is understood to be in the physical domain.

Stator sound field

As shown previously^{3,4}, application of generalized functions to make Eqs.(1-2) formally valid throughout space, i.e. also within the blades, and elimination of the velocity yields a non-homogeneous convected-wave equation in the pressure. The right hand side of this equation consists of two source terms, one of which contains the blade loading distribution and the other the blade thickness distribution. It appears that the latter only affects the steady blade response and plays no role in the wake interaction problem. After the construction of Green's function \tilde{G} for this equation in terms of a multiple Fourier transform, the wake interaction pressure field of a stator can be expressed as the following integral over the source volume and time

$$\bar{p} = \iiint \langle \nabla_0 \tilde{G} \cdot \nabla S \rangle \bar{p} \delta(S) d\xi d\tau \quad (3)$$

where ∇_0 denotes the gradient operator with respect to the source coordinates. Following Ffowcs Williams and Hawkings⁴, S is a smooth function that defines the vane surfaces through $S > 0$ outside and $S < 0$ inside the vanes. This pressure field contains unsteady components at multiples of the rotor wakes passing frequency. Upon substitution of the pressure field, the momentum equation yields expressions for the velocity induced by the vane loading. After omitting the higher order terms in the geometry, upper and lower surface pressure reduce into the pressure jump Δp across the vanes.

Integral equation

To solve the unknown pressure jump distribution Δp we have to apply the boundary condition of flow tangency at the vane surfaces. By splitting the incident field of rotor wakes into circumferential Fourier components, the integral equation becomes identical for all vanes of the stator. Combining the boundary conditions at upper and lower blade surfaces as in Ref.3, we obtain an integral equation for Δp due to an incident velocity field. The numerical method to solve this integral equation is described in Refs.5 and 6.

Modal amplitudes

Green's function \tilde{G} can be considered as the sound field of an impulsive point source. For a duct \tilde{G} takes the form of an expansion in acoustic modes⁶. For unleaned vanes, the resulting pressure field at a single frequency can be written as

$$\begin{aligned} \bar{p}(x, r, \theta, t) = & \frac{-B}{2\pi} \exp(i\omega t) \sum_{n=-\infty}^{\infty} \exp[in(\theta-D)] \\ & \times m \sum_{\mu=1}^{\infty} \frac{U_{m\mu}(r)}{2\beta_{m\mu}(\omega)} \int_h^1 \frac{U_{m\mu}(\rho)}{\rho} \int_{x_L(\rho)}^{x_T(\rho)} \Delta p(\xi, \rho) \\ & \times \exp \left[i \frac{(x-\xi)}{\beta^2} [M\omega - \text{sgn}(x-\xi)\beta_{m\mu}(\omega)] \right] d\xi d\rho \end{aligned} \quad (4)$$

where the circumferential wave number $m = k-nB$ and

$$\begin{aligned} \beta_{m\mu} &= \omega \sqrt{1 - (\varepsilon_{m\mu}\beta/\omega)^2} & \text{if } (\varepsilon_{m\mu}\beta)^2 \leq \omega^2 \\ \beta_{m\mu} &= -i \sqrt{(\varepsilon_{m\mu}\beta)^2 - \omega^2} & \text{if } (\varepsilon_{m\mu}\beta)^2 > \omega^2 \end{aligned} \quad (5)$$

It is well known¹ that for a given frequency ω , only a finite number of modes actually propagates along the duct. In practice it is quite feasible to select blade and vane numbers such that in the blade passing frequency (1st harmonic) all modes are cut-off, i.e. not propagating. Similarly, in many practical cases only a single term of the n -series is propagating in the second harmonic. If the corresponding m for this term can be made zero, no sound will radiate in this frequency. However, at this point it is to be remembered that the present analysis is concerned with the leading term of an asymptotic analysis in the small perturbation parameter. Therefore, higher order terms have to be taken into account if the leading term vanishes. For instance, it should be noted that the vane geometry is to leading order approximated by flat plates parallel to the axial mean flow. In an earlier study² the, higher order, effect of vane camber and stagger was shown to become significant in the case of high frequencies and low m 's. In this paper it is shown that even with a truly flat geometry the sound will not vanish when $m = 0$.

Leading edge suction force

Vanes are designed to operate under a wide range of angles of attack in a subsonic flow and therefore have a rounded leading edge which will sustain a suction force in the forward direction. In a perturbation analysis this suction is a higher order effect which, for instance, restores zero drag for a plate under an angle of attack in a subsonic, inviscid flow.

In principle the leading edge suction force is not captured by the lifting surface approximation, which accommodates only forces normal to the lifting surface. However, the suction force can be recovered from a local application of the steady, two-dimensional potential theory for a semi-infinite plate. In dimensional form

the complex potential χ of a semi-infinite plate in a parallel flow Ui_x with superimposed circulation γ is given by

$$\chi = U(z + \gamma\sqrt{z}) \quad (6)$$

Hence the complex conjugate velocity is (Fig. 1)

$$u - iv = \frac{d\chi}{dz} = U \left[1 + \frac{\gamma}{2\sqrt{r}} \exp(-i\frac{\phi}{2}) \right] \quad (7)$$

Applying Bernoulli's theorem for incompressible flow

$$p + \frac{1}{2}\rho_{\infty}(u^2 + v^2) = p_{\infty} + \frac{1}{2}\rho_{\infty}U^2 \quad (8)$$

along the upper (-) and lower (+) surface of the plate yields

$$\Delta p(x) = p^+ - p^- = \frac{1}{2}\rho_{\infty}U^2 \frac{2\gamma}{\sqrt{x}} \quad (9)$$

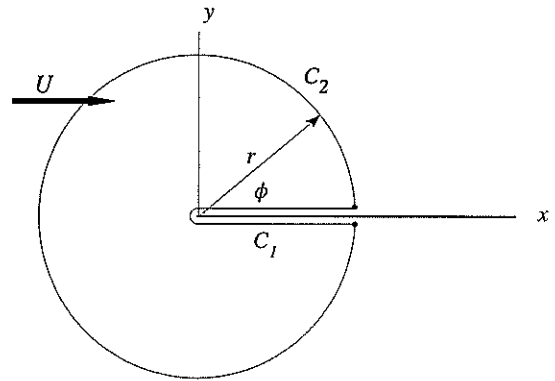


Fig.1 Integration contours to recover suction force

Now consider a contour C_1 wrapped around the plate leading edge (Fig.1). From the Blasius theorem⁷ it follows that the net force (X, Y) acting on the covered part of the plate is given by

$$X - iY = i \frac{\rho_{\infty}}{2} \int_{C_1} \left[\frac{d\chi}{dz} \right]^2 dz \quad (10)$$

Obviously, the integrand has singularities in $z = 0$, but since the contour made up by C_1 and C_2 does not enclose any singularity we have

$$\int_{C_1} \left[\frac{d\chi}{dz} \right]^2 dz = - \int_{C_2} \left[\frac{d\chi}{dz} \right]^2 dz \quad (11)$$

Hence the force on the forward part of the plate can

equivalently be calculated from the integration along C_2 , which is straightforward.

The resulting suction force X is given by

$$X = -\frac{1}{2}\rho_\infty U^2 \frac{\pi}{2} \gamma^2 \quad (12)$$

Substitution of Eq.(9) into Eq.(12) to eliminate the circulation γ and application of the Prandtl-Glauert correction factor for linear compressibility yields the following non-dimensional formulation

$$C_s = \frac{\pi}{4} \frac{c}{2} \frac{1}{(\cos\Lambda)^2} \lim_{s \rightarrow 0} \left[\sqrt{s} \Delta C_p(s) \right]^2 \quad (13)$$

where s denotes the local chordwise coordinate (scaled on the semi-chord). It is to be noted that U in Eq.(12) is the x -wise velocity in a plane normal to the leading edge. This explains the appearance of the local sweep angle Λ of the vane leading edge in Eq.(13).

Frequency doubling

In the previous section, a theory for steady flow was applied on a very small length and time scale (in the vicinity of the leading edge) to recover the suction force. On the larger scale of the complete blade row, however, the suction force is time-dependent since the pressure jump fluctuates. Making the time dependence explicit by replacing ΔC_p in Eq.(13) by $\Delta C_p \cos(\omega t + \phi)$ we obtain

$$\bar{C}_s(t) = \frac{1 + \cos[2(\omega t + \phi)]}{2} C_s \quad (14)$$

This remarkable result shows that the suction force resulting from a pressure jump oscillating with a frequency ω splits itself into a steady part and a part oscillating with frequency 2ω . Consequently, the 1st harmonic pressure jump generates a suction force in the 2nd harmonic, the 2nd harmonic pressure jump generates a suction force in the 4th harmonic, etc..

This is a truly nonlinear effect that is not present in 1st order acoustic theories, even in those that account for mean vane loading and non-uniform mean flow. The reason of the frequency doubling is that the suction phenomenon is insensitive to the sign of angle of attack; upwash is as effective as downwash.

Note that this frequency-doubling does not occur when the flow separates at the leading edge and forms a vortex. In that case the suction analogy^{5,8,9} applies with a leading edge force acting normal to the lifting surface and oscillating at the same frequency as the associated ΔC_p .

To compute the contribution of the suction force in the modal amplitude we have to go back to Eq.(3). Substi-

tution of Eq.(14), in which 2ω is understood to be equal to ω in Eq.(15), yields after some manipulation

$$\begin{aligned} \Delta A_{m\mu}^\pm &= -\frac{B}{4\pi} \frac{M^2}{2} \frac{1}{\beta_{m\mu}(\omega)} \\ &\times \int_h^1 \exp \left[-ix_L \frac{M\omega - \text{sgn}(x-x_L)\beta_{m\mu}(\omega)}{\beta^2} \right] \\ &\times \left[\frac{M\omega - \text{sgn}(x-x_L)\beta_{m\mu}(\omega)}{\beta^2} U_{m\mu}(\rho) \cos\Lambda \right. \\ &\quad \left. - i U_{m\mu}'(\rho) \sin\Lambda \right] C_s(\rho) d\rho \end{aligned} \quad (15)$$

Parametric study

Configuration

To obtain an idea of the relevance of the suction phenomenon, its effect for a generic modern fan was numerically studied. The characteristics of this fan are listed in Table 1. The stator has vanes with a constant chord, without sweep and lean. The rotor has unswept blades with a constant axial extent aligned with the relative local main flow. In the present study the rotor is considered as an acoustically transparent, viscous wake generator.

To put the analysis in the practical context of noise control, the effect was studied as a function of the axial gap between rotor and stator. Increasing the rotor-stator spacing is an obvious way to reduce interaction noise.

Table 1 Rotor & stator data

Number of rotor blades	23
Number of stator vanes	var.(45-47)
Hub/tip ratio, h	0.50
Vane chord length	0.12
Axial Mach number	0.32
Rotor tangential tip Mach No.	0.75
Axial extent rotor chord	0.15
Rotor blade drag coefficient	0.025/0.05
Nondim. 2nd harm. freq.	34.50
Speed of sound (m/s)	340.43
Air density (kg/m ³)	1.225

Wake velocity

Incident rotor blade wakes were computed according to Schlichting's¹⁰ formulas for turbulent wakes in a quasi-two-dimensional way. In a local, Cartesian coordinate system (s, q) with the rotor blade trailing edge as origin the wake velocity is given by

$$w = -\frac{U}{4\sqrt{\pi\lambda}} \sqrt{\frac{c_{dw} c_w}{s}} \exp\left[\frac{-q^2}{4\lambda c_{dw} c_w s}\right] \quad (16)$$

where c_{dw} is the local drag coefficient, c_w the local rotor blade chord and the empirical coefficient $\lambda = 0.0222$. This wake profile is for isolated wakes and has no definite boundaries. Since we are dealing with a multi-blade wake system, wake merging will take place at some downstream location. In anticipation of merging we also consider a periodic cosine velocity profile, satisfying the far-wake momentum relation, as follows

$$w = -\frac{U}{2} \sqrt{\frac{c_{dw} c_w}{s}} \left[\cos\left(\frac{2\pi q}{\sqrt{c_{dw} c_w s}}\right) + 1 \right] \quad (17)$$

with boundaries

$$q = \pm \frac{1}{2} \sqrt{c_{dw} c_w s} \quad (18)$$

Beyond the location where the boundaries of adjacent wakes intersect, the wake width cannot further increase and, following Schlichting, the next wake profile is adopted

$$w = -\frac{U}{2} \sqrt{\frac{c_{dw} c_w s_m}{s}} \left[\cos\left(\frac{2\pi q}{\sqrt{c_{dw} c_w s_m}}\right) + 1 \right] \quad (19)$$

where the subscript m refers to the merging station. Two levels of incident wake strength were investigated: a rotor blade drag coefficient of 0.025 ("low") and of 0.050 ("high").

Low drag rotor wakes

All acoustic intensity mentioned below refers to the second harmonic of the rotor blade passing frequency only. The presumably much weaker higher harmonics are not considered.

The fan has 23 rotor blades and with a stator of 46 vanes Eq.(4) predicts a vanishing base acoustic level in the 2nd harmonic. Hence the acoustic intensity for this case in Fig.2 is solely caused by the suction force. Since this force is chordwise compact, there is no difference between upstream and downstream intensity. The "suction noise" only weakly decreases as the axial

gap between rotor and stator is increased. It takes about a 6-fold gap increase to obtain a reduction of 10 dB.

If the number of vanes is increased to 47, cut-on modes with $m = -1$ are generated in the 2nd harmonic. The minus sign indicates that these modes are counter-rotating to the rotor. However, to isolate the suction effects, rotor shielding¹¹, although important in practice, was not taken into account in the present analysis. In Fig.3 the computed upstream acoustic intensity is presented. For a small gap the suction effect is small but beyond a gap of 0.4 duct radius it is prominent. A maximum of 9 dB in the suction effect is observed at a gap of 0.6.

As shown in Fig.4, the base level of the downstream interaction noise is about 6 dB higher than the upstream level. Hence, the suction effect is relatively weaker than upstream (cf. Fig.3) and never more than 3 dB, which is still significant, of course.

If the number of vanes is decreased to 45, $m = 1$ modes, rotating in the same sense as the rotor, are generated in the second harmonic. In Fig.5 the resulting upstream acoustic intensity is given. Despite the slightly lower number of vanes, the base level for a narrow gap is about 5 dB higher than for the $m = -1$ case in Fig.3. This shows, once more, how sensitive the acoustic response can be to details one might intuitively ignore. Similar to the $m = -1$ case, the suction effects becomes more important as the gap increases. At a gap of 0.7 the suction effect is 10 dB. The relative increase of the suction effect for a larger gap corresponds to merging of the rotor wakes, which favors the first wake harmonic. As shown in Fig.6, the downstream acoustic intensity is modified by suction by 3 dB at most.

High drag rotor wakes

The effect of a larger drag coefficient of the rotor blades is not simply a linear scaling of the incident velocity. As shown by Eqs.(16) and (17), before merging drag affects both the wake velocity and the wake width. The latter is directly connected with the harmonic content of the incident wake system. Since the suction force scales on the square of the response on the first wake harmonic and the base acoustic level on the response on the second wake harmonic, the net acoustic effect of a drag increase is virtually unpredictable by simple reasoning and has to be computed.

In Fig.7 computation shows (cf. Fig.2) that the suction effect is about 10 dB stronger at a gap of 0.1 while the level at a gap of 0.8 has hardly changed. This is not unexpected since a higher drag coefficient will enhance the first wake harmonic close to the rotor. At larger distances the first harmonic will dominate anyway as a

result of wake merging.

As shown in Fig.8 (cf. Fig.3) the increased suction force is quite effective in the upstream intensity for the $m = -1$ case since the base acoustic level has become lower. A suction effect of more than 5 dB at the smallest gap and more than 9 dB at a gap of 0.4 is really significant since the gap range below 0.4 is common practice. For a gap larger than 0.4 the suction effect gradually diminishes.

The downstream intensity for $m = -1$ is shown in Fig.9. The suction effect is clearly present but not as spectacular as in the upstream case. Still, an effect of 3 dB at a gap of 0.4 is remarkable since the effect for the low c_d in Fig.4 is negligible at the same gap. Note also the much steeper initial gradient at which the intensity decreases. Despite a drag coefficient twice as high, this results in a lower noise output in the practically important gap range between 0.2 and 0.5.

The upstream results for 45 vanes ($m = 1$) are shown in Fig.10. The maximum suction effect is 8 dB at a gap of 0.4. Here also the interaction noise of the high drag rotor is less than the noise of the low drag rotor (Fig.5) for a gap between 0.2 and 0.5.

Finally, the downstream acoustic intensity in Fig.11 shows a maximum suction effect of 2.7 dB at a gap of 0.4. Also in this case the gap range 0.2-0.5 is quieter for the high drag rotor (cf. Fig.6).

Concluding remarks

An analysis of the acoustic effect of vane leading edge suction has been presented.

This effect is a genuinely nonlinear phenomenon that involves frequency doubling.

It has been outlined how the suction force can be recovered from the first order, lifting surface theory.

A numerical study for a generic fan shows that the suction effect provides a realistic bottom level for otherwise vanishing modal amplitudes ($m=0$).

For non-vanishing modal amplitudes ($m \neq 0$), the influence of the suction force tempers the beneficial effect of a large rotor-stator spacing. The suction effect can modify the acoustic intensity by as much as 10 dB.

For low drag rotor wakes the suction effect on acoustic intensity is only significant for rotor-stator gaps larger than 0.4 duct radius.

For high drag rotor wakes the suction effect on acoustic intensity is significant for small gaps as well. A maximum effect is observed at a gap of about 0.4.

For the configuration studied, an increase in rotor blade drag can reduce the interaction noise within a certain gap range.

References

- ¹Tyler, J.M., Sofrin, T.G., "Axial Flow Compressor Noise Studies," *SAE Transactions*, Vol.70, 1962, pp. 309-332.
- ²Schulten, J.B.H.M., "Vane Stagger Angle and Camber Effects in Fan Noise Generation", *AIAA Journal*, Vol.22, No.8, 1984, pp. 1071-1079.
- ³Schulten, J.B.H.M., "Effects of Asymmetric Inflow on Near-Field Propeller Noise," *AIAA Journal*, Vol.34, No.2, Feb. 1996, pp. 251-258.
- ⁴Ffowcs Williams, J.E., Hawkings, D.L., "Sound generation by turbulence and surfaces in arbitrary motion," *Philosophical Transactions of the Royal Society of London*, Series A, Vol.264, 1969, pp. 321-341.
- ⁵Schulten, J.B.H.M., "Advanced Propeller Performance Calculation by a Lifting Surface Method," *Journal of Propulsion and Power*, Vol.12, No.3, May-June 1996, pp. 477-485.
- ⁶Schulten, J.B.H.M., "Vane sweep effects on rotor/stator interaction noise," *AIAA Journal*, Vol.35, No.6, 1997, pp.945-951.
- ⁷Milne-Thomson, L.M., *Theoretical Aerodynamics*, Dover Publications, New York, 1973.
- ⁸Polhamus, E.C., "A Concept of the Vortex Lift of Sharp-Edge Delta Wings Based on a Leading-Edge-Suction Analogy," NASA TN D-3767, 1966.
- ⁹Lamar, J.E., "Prediction of Vortex Flow Characteristics of Subsonic and Supersonic Speeds," *Journal of Aircraft*, Vol.13, No. 7, July 1976, p.490 - 494.
- ¹⁰Schlichting, H., *Boundary Layer Theory*, McGraw-Hill, New York, 1979, Ch.24.
- ¹¹Schulten, J.B.H.M., "Sound transmission through a rotor," *Proceedings DGLR/AIAA 14th Aeroacoustics Conference* (Aachen, Germany), Vol.I, Deutsche Gesellschaft für Luft- und Raumfahrt, Bonn, Germany, 1992, pp. 502-509.

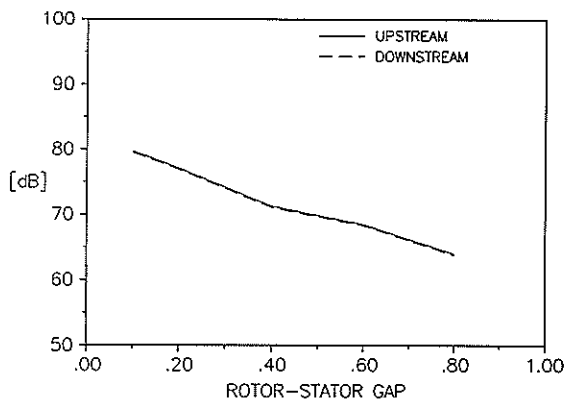


Fig. 2 Acoustic intensity due to leading edge suction, $m=0$, 46 vanes, rotor $c_d = 0.025$.

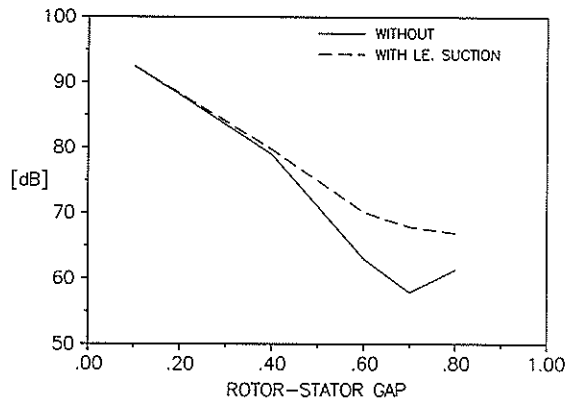


Fig. 5 Upstream intensity, $m = 1$ (45 vanes), rotor $c_d = 0.025$.

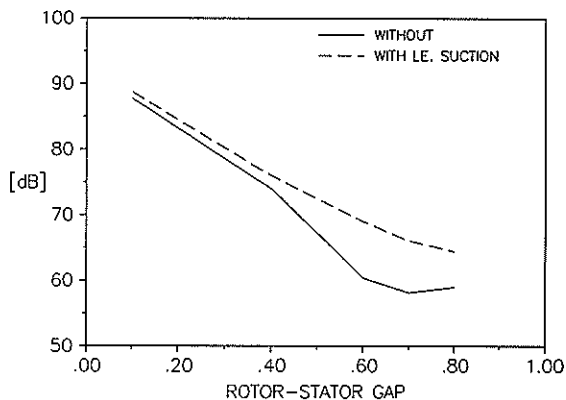


Fig. 3 Upstream intensity, $m=-1$ (47 vanes), rotor $c_d = 0.025$.

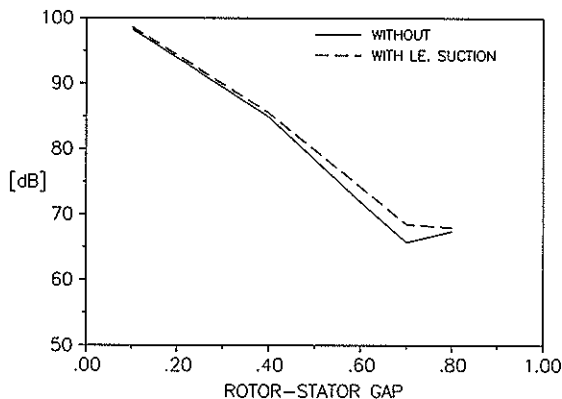


Fig. 6 Downstream intensity, $m = 1$ (45 vanes), rotor $c_d = 0.025$.

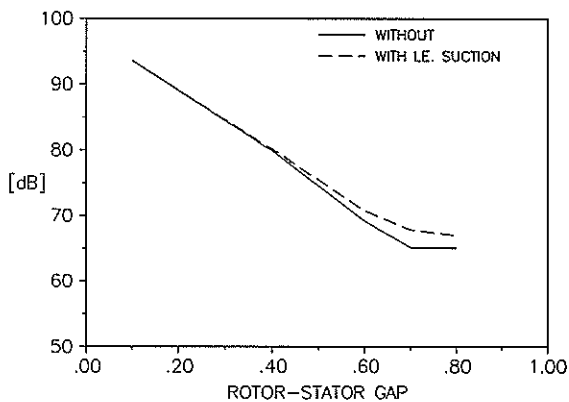


Fig. 4 Downstream intensity, $m=-1$ (47 vanes), rotor $c_d = 0.025$.

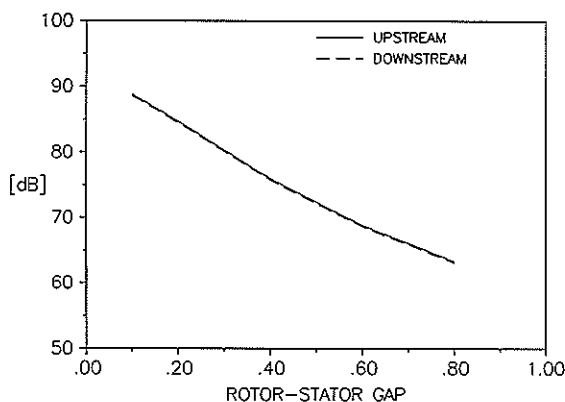


Fig. 7 Effect of increased rotor blade drag ($c_d = 0.05$) on acoustic intensity for $m = 0$ (46 vanes).

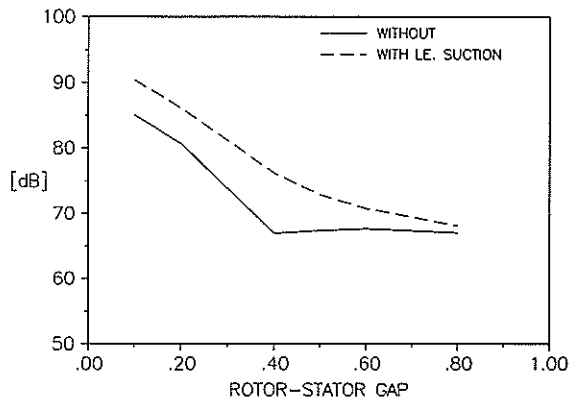


Fig.8 Upstream intensity, $m = -1$ (47 vanes), rotor $c_d = 0.05$.

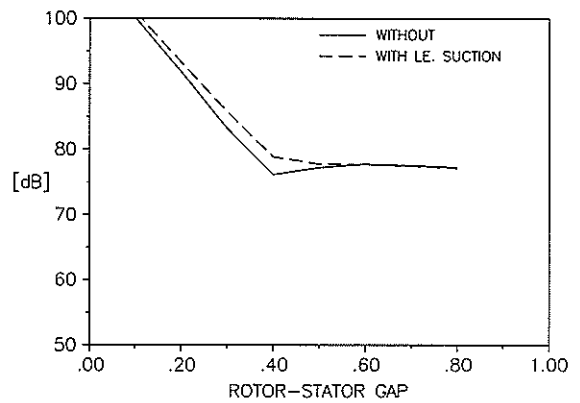


Fig.11 Downstream intensity, $m = 1$ (45 vanes), rotor $c_d = 0.05$.

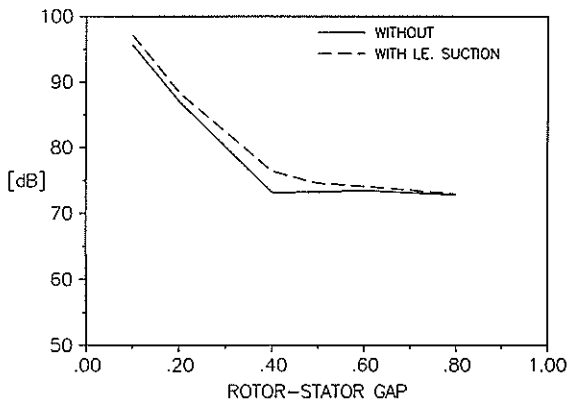


Fig.9 Downstream intensity, $m = -1$ (47 vanes), rotor $c_d = 0.05$.

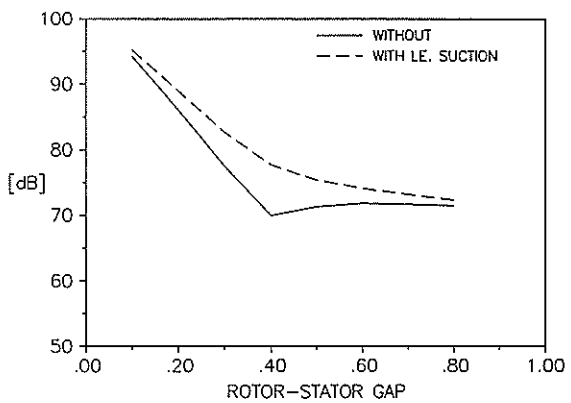


Fig.10 Upstream intensity, $m = 1$ (45 vanes), rotor $c_d = 0.05$.